JACS
JOURNAL OF THE AMERICAN CHEMICAL SOCIETY
Article
pubs.acs.org/JACS

Drug Resistance Conferred by Mutations Outside the Active Site through Alterations in the Dynamic and Structural Ensemble of HIV-1 Protease

Debra A. Ragland, Ellen A. Nalivaika, Madhavi N. L. Nalam, Kristina L. Prachanronarong, Hong Cao, Rajintha M. Bandaranayake, Yufeng Cai, Nese Kurt-Yilmaz, and Celia A. Schiffer*

Department of Biochemistry and Molecular Pharmacology, University of Massachusetts Medical School, Worcester, Massachusetts 01605, United States

Supporting Information

ABSTRACT: HIV-1 protease inhibitors are part of the highly active antiretroviral therapy effectively used in the treatment of HIV infection and AIDS. Darunavir (DRV) is the most potent of these inhibitors, soliciting drug resistance only when a complex combination of mutations occur both inside and outside the protease active site. With few exceptions, the role of mutations outside the active site in conferring resistance remains largely elusive. Through a series of DRV–protease complex crystal structures, inhibition assays, and molecular dynamics simulations, we find that single and double site mutations outside the active site often associated with DRV resistance alter the structure and dynamic ensemble of HIV-1 protease active site. These alterations correlate with the observed inhibitor binding affinities for the mutants, and suggest a *network hypothesis* on how the effect of distal mutations are propagated to pivotal residues at the active site and may contribute to conferring drug resistance.

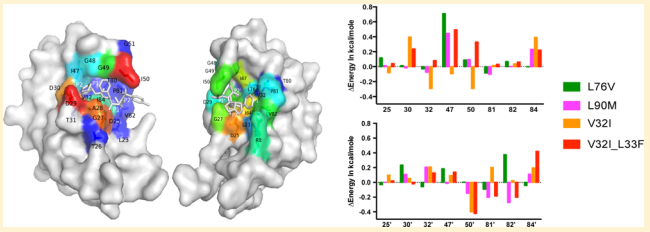

INTRODUCTION

In the absence of a vaccine and in lieu of a cure, antiretroviral combination therapy has been the main form of treatment for individuals infected with HIV. As is the case with treatment of most rapidly evolving viruses/diseases, drug resistance decreases the effectiveness of treatment. The high replicative capacity of HIV and the infidelity of the reverse transcriptase quickly lead to a heterogeneous population of viruses within patients, from which resistance has emerged to all 30 of the currently used antiviral drugs.

HIV-1 protease inhibitors (PIs) have recently emerged as the most effective drugs in the treatment of HIV.[1−3] PIs are competitive active site inhibitors that mimic the transition state of the enzyme and are the most potent antiretroviral drugs for the treatment of HIV/AIDS.[4] These drugs are ideal for therapy as they target the viral protease responsible for viral maturation and thus the spread of the virus. Unfortunately, the rapid evolution of HIV-1, coupled with the selective pressure of therapy, results in many viable multidrug resistant variants. In fact, mutations at 45 of the 99 residues that make up HIV-1 protease have been implicated in drug resistance.[5] While resistance due to mutations at 11 of these 45 residues can be explained as direct changes within the active site, the resistance mechanisms for the majority of the remaining mutations outside the active site of the enzyme mostly remain elusive.

Drug resistance mutations in HIV-1 protease allow the enzyme to become less susceptible to inhibition while retaining enzymatic activity. Points of inhibitor–protease contact at residues within the active site where the inhibitor protrudes beyond the substrate envelope are sites selected for resistance, as their interactions are more critical for inhibitor binding than substrate turnover.[6] While mutations at some active site residues, such as 82 and 84, lead to resistance to all PIs, other mutations are signatures of specific inhibitors, such as D30N for nelfinavir and I47A for lopinavir.[7] These mutations directly impact inhibitor binding by altering or reducing contacts necessary for inhibiting the enzyme, but can also simultaneously decrease the catalytic efficiency or enzymatic fitness. The mutations at the remaining 34 of the 45 residues associated with drug resistance occur outside the active site. These changes have often been considered secondary or accessory mutations, and are thought to indirectly impact inhibitor binding while assisting in enzyme fitness or stability. Structural studies on the effect of several HIV-1 protease secondary mutations have provided insights into how inhibitor binding may be affected.[8−12] However, for the most part, their specific role in protease inhibitor resistance or mechanism of action has not been elucidated.

Darunavir (DRV) is the most potent of the United States Food and Drug Administration (FDA) approved HIV-1 protease inhibitors. This high potency combined with the inhibitor's fit within the substrate envelope appears to account for DRV's robustness against drug resistance.[13,14] Drug

Received: April 24, 2014
Published: August 4, 2014

   dx.doi.org/10.1021/ja504096m | J. Am. Chem. Soc. 2014, 136, 11956−11963

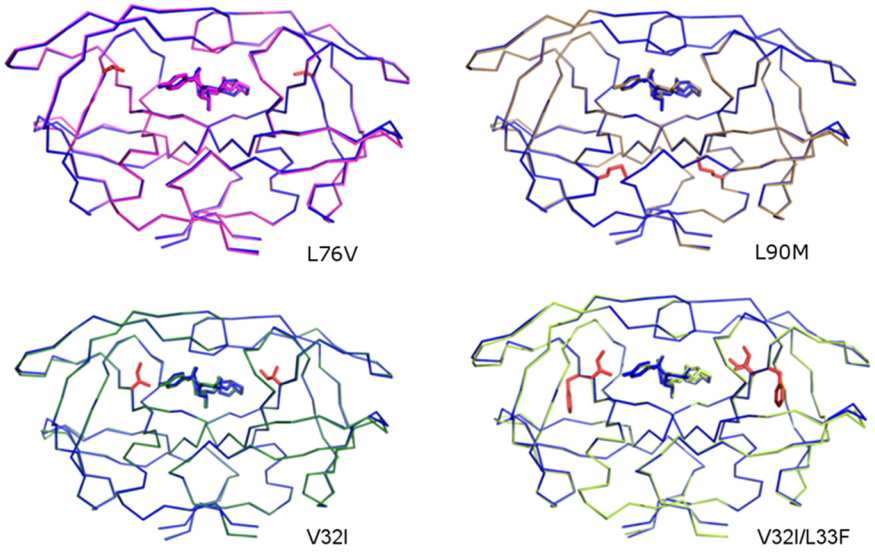

Figure 1. Structure of HIV-1 protease variants bound to DRV. Crystal structures of mutant protease variants superimposed with the WT protease complex structure in blue. The side chains of mutation sites are in red sticks.

resistance to DRV usually occurs only in patients who have high levels of pre-existing PI resistance, requiring at least seven mutations to simultaneously occur for therapeutic failure. In fact, DRV is being investigated as a potential monotherapy in treatment-naïve patients.[15]

In DRV-resistant HIV variants, many changes occur outside the active site of the enzyme in complex combinations. Single site mutations cannot confer high levels of resistance to DRV, and a combination of multiple mutations including those outside the active site are needed to decrease potency. However, the role of these mutations in conferring resistance is not well understood: some may be enhancing enzymatic activity, while others may directly confer drug resistance and still others may be residual mutations from previous therapy history. In this study, we examine some of the most common of these mutations, V32I, L33F, L76V, and L90M (as a control; not a signature of DRV resistance but frequent in multidrug resistance[10]), for their impact on DRV inhibition. Using a combination of static and dynamic structural analyses, by determining crystal structures of complexes and performing molecular dynamics simulations, we elucidate the possible roles of these secondary mutations both independently (L76V, L90M, V32I) and in combination (V32I/L33F) in conferring resistance. We find how mutations at residues with no direct contact with the inhibitor can alter the structure and dynamics of the protease to affect inhibitor binding through common mechanisms, which we define through a "network hypothesis".

RESULTS

To determine how mutations remote from the active site contribute to DRV resistance in HIV-1 protease, the impact of four mutations (L76V, L90M, V32I, and V32I/L33F; Figure 1) in a subtype B background was investigated in terms of enzyme inhibition, inhibitor-bound crystal structures, and molecular dynamics simulations.

Enzyme Inhibition. The enzyme inhibition constant for DRV was measured against each of the protease mutants, in addition to WT subtypes B and C for comparison (Table 1). DRV is highly potent against WT subtype B protease with a K_i of 2 pM, as we previously reported.[13] The level of inhibition for the mutants varied from 2 pM to 45 pM, with the L90M mutant being inhibited as potently as the WT protease and the V32I/L33F double mutant exhibiting the greatest decrease in susceptibility to DRV with a fold-change greater than 20. Hence, single mutations are not enough to confer high levels of DRV resistance, as expected, and the mutations had varying degrees of effects on DRV susceptibility.

Table 1. DRV Interaction and Susceptibility of HIV-1 Protease Variants[a]

protease variant	K_i (pM)	vdW (kcal/mol)	ΔvdW (kcal/mol)
subtype C	5 ± 2 (2.5)		
WT	2 ± 1 (1.0)	−44.5	
L76V	3 ± 2 (1.5)	−43.0	1.5
L90M	2 ± 2 (1.0)	−44.4	0.1
V32I	7 ± 9 (3.5)	−44.2	0.2
V32I/L33F	45 ± 18 (22.5)	−43.3	1.2

[a]DRV inhibition constants (K_i) of HIV-1 protease variants, with fold-changes relative to subtype B WT protease in parentheses. The overall vdW interaction energy between the inhibitor and protease was determined from crystal structures.

Crystal Structures. To structurally characterize the effects of the mutations on DRV binding, we determined the crystal structures of variants L76V, L90M, V32I, and V32I/L33F, which diffracted to resolutions of 1.5−1.9 Å in the $P2_12_12_1$ space group (Table 2). Alignment of the four complex structures on our previously determined structure of the WT protease−DRV complex (1T3R[16]) showed that the variants had only minor backbone variations, mainly in the 20s loop likely due to crystal packing differences (Figure 1). Therefore, the mutations had very little impact on the overall backbone structure of the protease.

Detailed Structural Analysis of DRV Binding from Cocrystal Structures. The high-resolution cocrystal structures enabled detailed analysis of protease−DRV contacts in each of the five complexes. The WT complex had the most extensive van der Waals (vdW) contacts with the inhibitor with a favorable energy of −44.5 kcal/mol, similar to V32I and L90M variants (Table 1). The L76V variant and V32I/L33F double mutant lost more than 1 kcal/mol in vdW contact

dx.doi.org/10.1021/ja504096m | J. Am. Chem. Soc. 2014, 136, 11956−11963

Table 2. Crystallographic Statistics for DRV-Bound HIV-1 Protease Structures

	WT[a]	L76V	L90M	V32I	V32I/L33F
PDB code	1T3R	3OY4	4Q1W	4Q1X	4Q1Y
data collection					
space group	$P2_12_12_1$	$P2_12_12_1$	$P2_12_12_1$	$P2_12_12_1$	$P2_12_12_1$
a (Å)	50.75	50.72	50.74	50.91	50.81
b (Å)	57.81	57.71	57.55	58.28	58.23
c (Å)	62.01	62.03	61.81	61.78	61.82
b-angle	90	90	90	90	90
Z	2	2	2	2	2
temperature (K)	190	100	100	100	100
resolution (Å)	1.20	1.76	1.85	1.90	1.50
total reflections	55 056	133 462	107 138	100 241	192 411
unique reflections	52 226	17 434	15 822	14 168	29 633
R merge (%)	3.8	8.5	6.4	6.3	4.8
completeness (%)	95.5	97.8	98.6	93.9	98.7
crystallographic refinement					
R value (%)	14.0	18.0	17.3	18.0	18.3
R free (%)	17.9	21.9	20.6	23.4	20.7
RMSD in:					
bond length (Å)	0.039	0.006	0.008	0.008	0.009
bond angles	1.593	1.572	1.342	1.474	1.497

[a]From Surleraux et al.[16]

energy with DRV relative to the WT complex. Thus, despite no large-scale changes in the protease backbone, subtle changes in repacking occurred around DRV in these two complexes to weaken protease interactions with the inhibitor. However, the extent of contacts lost with DRV in the mutant crystal structures with respect to WT protease does not correlate completely with the fold-change loses in K_i values (Table 1).

Contacts involving specific DRV moieties (Figure 2) and protease active site residues (Figure 3) were analyzed in detail. In general, the impact of mutations on DRV contacts are larger at the P2 and P2′ than the central P1 and P1′ moieties. The bis-THF group of DRV P2 moiety forms the most extensive contacts in all of the complexes (Figure 2), but also loses considerable contacts due to the mutations, except in the V32I structure. In the case of V32I, DRV contacts are retained as in the WT complex, consistent with no significant change in total vdW or K_i values (Table 1). When this mutation occurs together with L33F in the double mutant though, contacts are lost in all three of P2, P1, and P2′ moieties. In the L90M variant, although interactions get weaker at the P2 position, gain of contacts at P1 compensate for this loss yielding comparable total vdW contacts and susceptibility to DRV as WT protease.

While the apo form of the protease is a symmetric homodimer, DRV induces asymmetry to the complex and thus despite identical residues mutating in both monomers, the effect of these mutations on protease−inhibitor contacts is distinct in the two monomers (Figure 3). Specifically, L76V and L90M mutations cause considerable loss of contacts at I47, but to a lesser extent at I47′. Other active site residues whose contacts are altered in mutant structures include I50 at the tip of the flaps, and 81−82−84 at the 80s loop. Contrary to previous reports,[17] we do not see any major enhancement of DRV contacts with the catalytic D25 in the L90M mutant, or any of the other 3 variants.

Residue 32 is at the periphery of the active site, and V32I mutation causes a unique pattern of rearrangement of inhibitor contacts than the other variants studied. Unlike L76V and

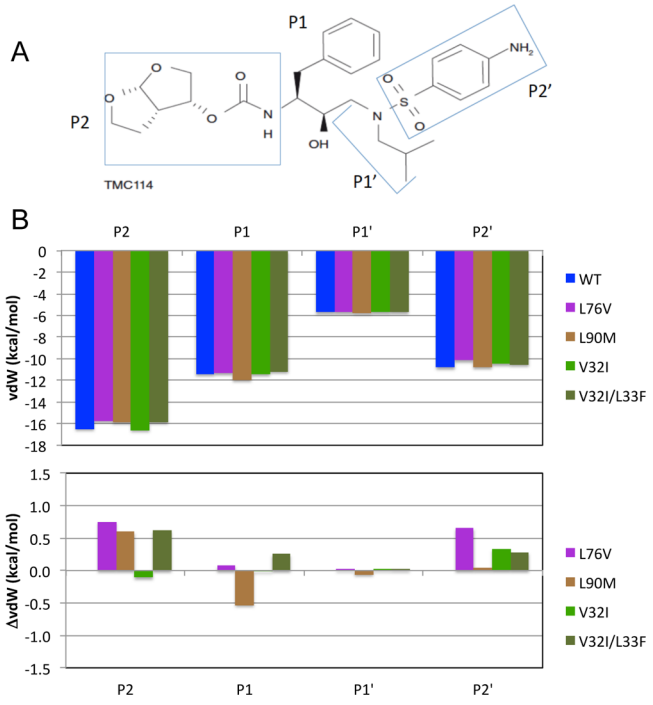

Figure 2. Contacts of DRV moieties with HIV-1 protease variants. (A) Chemical structure of DRV (TMC114) with the inhibitor moieties P2−P2′ indicated. (B) vdW interaction energy (kcal/mol) of DRV moieties for contacts with the protease active site in the crystal structures, and changes in vdW interaction energy in mutant structures relative to the WT complex. Positive values indicate loss of contacts.

L90M, contacts with 47 are retained in V32I. Although the backbone is not shifted significantly, the proximity of residue 32 to the 80s loop causes subtle rearrangements to result in repositioning of the DRV away from I84's and more toward I50s at the tip of the flaps. As a result, DRV contacts with residues 84, 81′, and 84′ are lost but those with 50 and 50′ are enhanced. The larger isoleucine also forms additional contacts

dx.doi.org/10.1021/ja504096m | J. Am. Chem. Soc. 2014, 136, 11956−11963

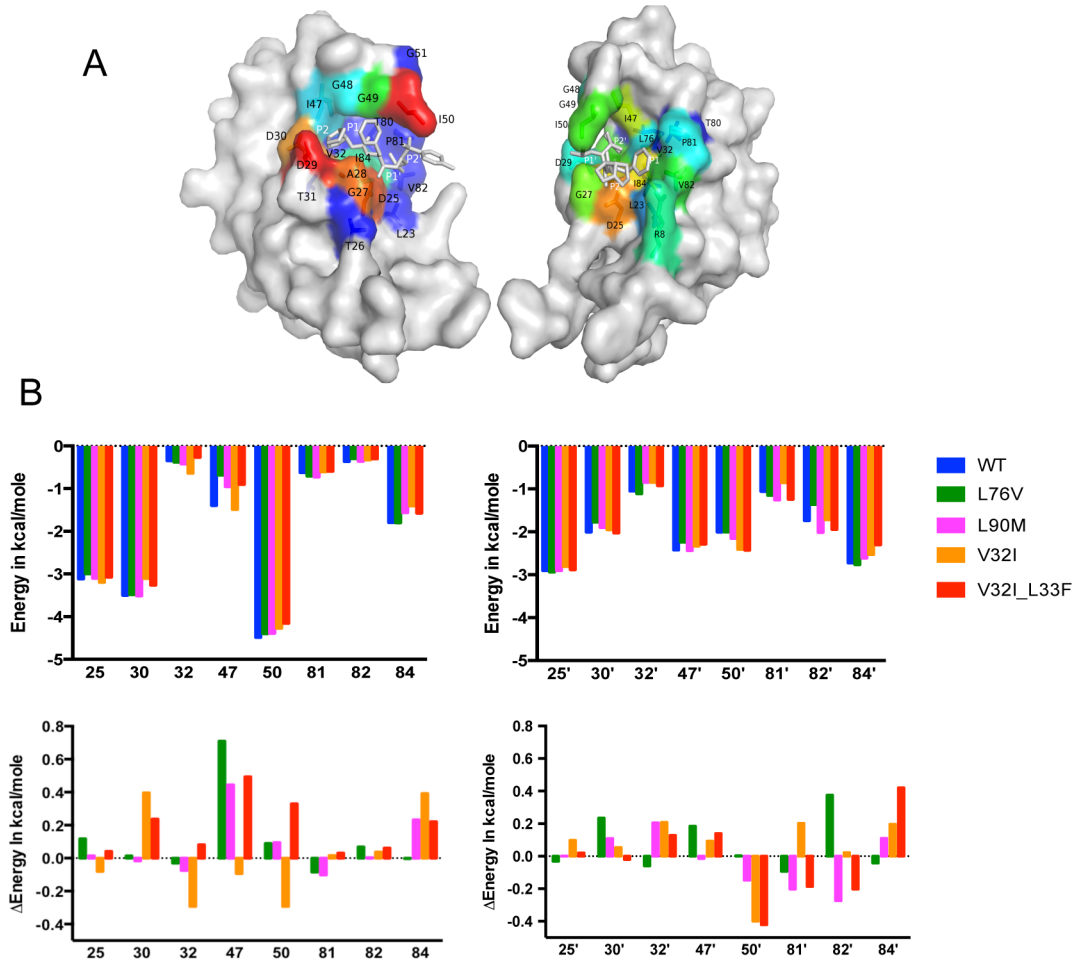

Figure 3. Contacts of protease active site residues with DRV in the crystal structures. (A) The two monomers of WT protease in surface representation with the bound DRV displayed as sticks. Active site residues are colored from blue to red for increasing vdW contacts with the inhibitor. The monomer that interacts mostly with the P2−P1 moieties of DRV is on the left, and the primed-side monomer is on the right. (B) The vdW interaction energy of active site residues in crystal structures (top), and changes in mutant complexes relative to the WT structure (bottom). Only the residues displaying considerable changes relative to WT are included for both monomers. See Figures S1 and S2 in the Supporting Information for all active site residues. Positive values indicate loss of contacts.

with the inhibitor in the unprimed-side monomer. In the V32I/L33F variant, which loses an additional 7-fold in binding affinity relative to V32I (Table 1), the contacts are rearranged again. In contrast with V32I alone, additional loss of interactions at residues 47 and 50 are observed. These losses of contacts are similar to the alterations observed in the L76V and L90M variants. Thus, the double mutant V32I/L33F variant alters the active site in a synergistic manner, leveraging both alterations similar to L76V and L90M, and some changes from V32I. The change in variants' affinity is not simply due to a loss of van der Waals contacts, but an interdependent change in optimal contacts.

In the WT complex, DRV forms a network of hydrogen bonds within the active site involving both backbone and side chains. Most of these bonds, including the two water-mediated ones with I50, are conserved in the variant complexes. Two exceptions occurred in the L76V and V32I complexes: Consistent with the loss of vdW contacts, in the L76V complex a hydrogen bond to the backbone of D30 is lengthened from 2.0 to 3.0 Å. In the V32I variant, an additional water-mediated hydrogen bond with the side chain of D30 is formed. Nevertheless, overall the hydrogen bonds with DRV within the various complexes are conserved.

Dynamic Simulations of Complexes. Analysis of crystal structures above revealed that the mutations away from the active site are able to influence interactions of DRV-contacting residues at the active site. The alterations in vdW contacts or hydrogen bonds lost, however, only partly correlate with the experimentally determined enzyme inhibition constants. Another possible mechanism by which these secondary mutations could alter inhibitor binding is by influencing the dynamic ensemble of the enzyme.

Starting from the crystal structures of the DRV complexes, three replicates of fully hydrated 10 ns MD simulations of each DRV complex were performed and analyzed. Root-mean-square deviations (RMSD) of Cα atoms during the simulation and the average root-mean-square fluctuations (RMSF) about their mean positions readily reveal that the secondary mutations alter the overall enzyme dynamics (Figure 4A). The L90M and V32I/L33F variants display larger fluctuations throughout the enzyme compared to the other variants, although the catalytic D25 stays relatively rigid in both monomers. These altered fluctuations are not restricted to the sites of mutation, but propagate throughout the enzyme.

To further analyze the impact of mutations on the dynamic ensemble sampled by the protease, the distance distributions

dx.doi.org/10.1021/ja504096m | J. Am. Chem. Soc. 2014, 136, 11956−11963

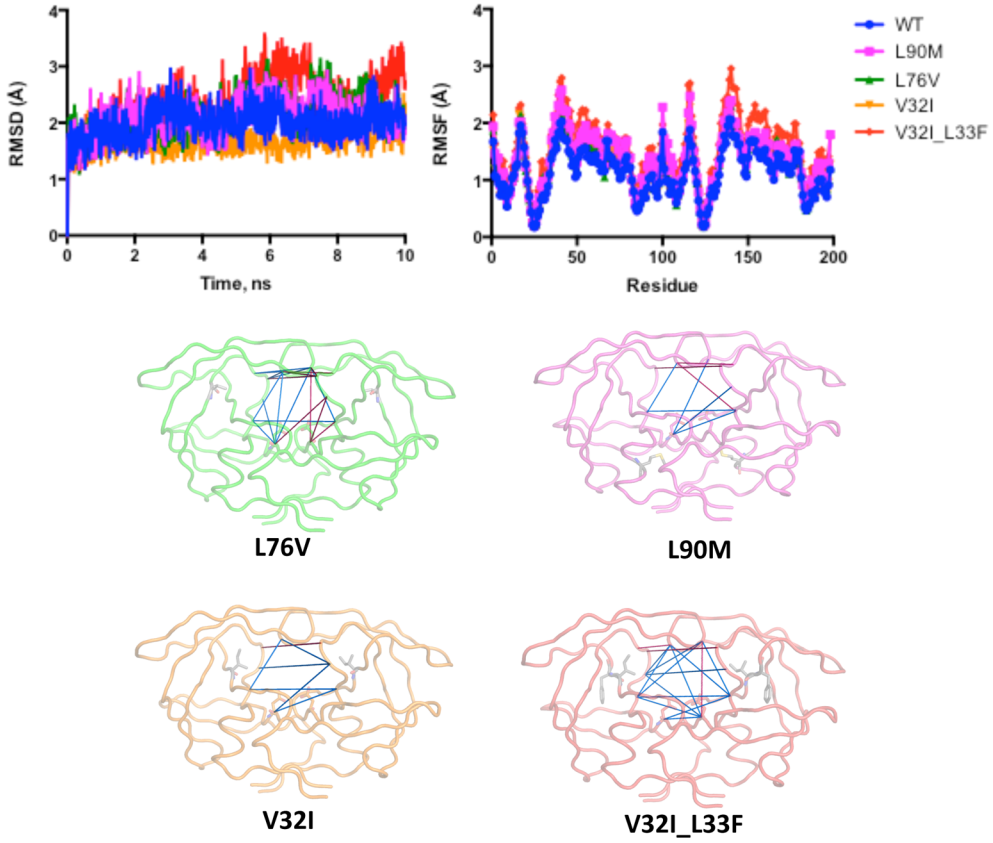

Figure 4. Molecular dynamics simulations of DRV–HIV-1 protease complexes. (A) RMSD of Cα atoms from the initial positions, and RMS fluctuations of residues averaged over three 10 ns trajectories. (B) Significantly altered change in distance between residue pairs around the active site relative to WT complex, sampled during the MD simulations; increased and decreased distances are indicated by blue and red, respectively. See Figure S3 for the distance distributions.

were calculated across the active site at a variety of positions (Figure 4B and Figure S3). In all the variant complexes, the dynamic ensemble sampled by the protease is altered relative to WT. Many of the distances displaying a significant change are longer than the WT distance, indicating a widening of the active site. In the L76V complex, the changes are highly asymmetric, with one side of the active site constricting and the other widening (Figure 4B). In all variant complexes, alterations involve residues in the 80s loops. The 80s loops in both monomers form the "side walls" of the active site. Relative to the WT complex, the distance between residues 81 in the two monomers are shorter, and that between 84–84′ are longer in all variants. Hence, the "upper" part of the side walls are closer and the "lower" part is farther away in the mutant complexes compared to the WT. In addition to the 80s loop, certain distances involving residue 50 at the tip of the flaps, and even the catalytic D25 are altered in the variant complexes. The catalytic site is the most invariant and dynamically restricted region of the protease, both when different crystal structures are compared and dynamics analyzed by simulations and NMR experiments.[18−20] Therefore, widening of the D25–D25′ distance in the V32I/L33F double mutant is an unusually profound impact of remote changes on the catalytic region.

The MD simulations also permitted a detailed analysis of the interaction network both for direct interactions within the active site to DRV and the internal hydrogen-bonding network throughout the enzyme (Figure 5, Figures S4–S6). Throughout the MD simulations the WT complex maintains a network of stable hydrogen bonds. Starting from the bottom of the enzyme the c-terminal α-helix forms a network of hydrogen bonds that links the termini of the protein to the flap regions. The backbone of residue 95 links to residue 90 which in turn contacts residue 86, residue 88 bridges to residues 29, 31, and 74, and residue 76 bonds to both residues 31 and 33 which is bonded to residue 78. Residues 29 and 30 make direct hydrogen bonds to DRV in both monomers. The hydrogen bonds linking residues 47 and 54 within the flaps stay tightly hydrogen bonded throughout the simulation. Thus, as we previously observed,[12] the hydrogen bonding network is stably retained within the WT MD simulation.

In comparing the simulations of the variant DRV complexes with the WT, subtle changes are seen in the vdW contacts within the active site (Figure S6), similar to what was observed in the crystal structures. However, in each of the four variants, with the notable exception of the 47–54 linkages, the hydrogen bond network is disrupted to a greater or lesser extent asymmetrically, including the direct hydrogen bonds with DRV (Figure 5B, S4, S5). The V32I/L33F variant is the most disrupted with 12 hydrogen bonds changing by greater than 20% relative to the WT complex throughout the dimer, with 11 being weakened (Figure 5D) including most dramatically the interactions of the side chain of Asn 88. Eight of these changes are within the monomer that coordinates the highly rigid bis-THF moiety including weakened interactions at points of contact between the protein and DRV. Thus, mutations distal to the active site often weaken the strength of the hydrogen bonds in the network, which is propagated through to the active site including altering vdW packing, pushing the flaps,

dx.doi.org/10.1021/ja504096m | J. Am. Chem. Soc. 2014, 136, 11956–11963

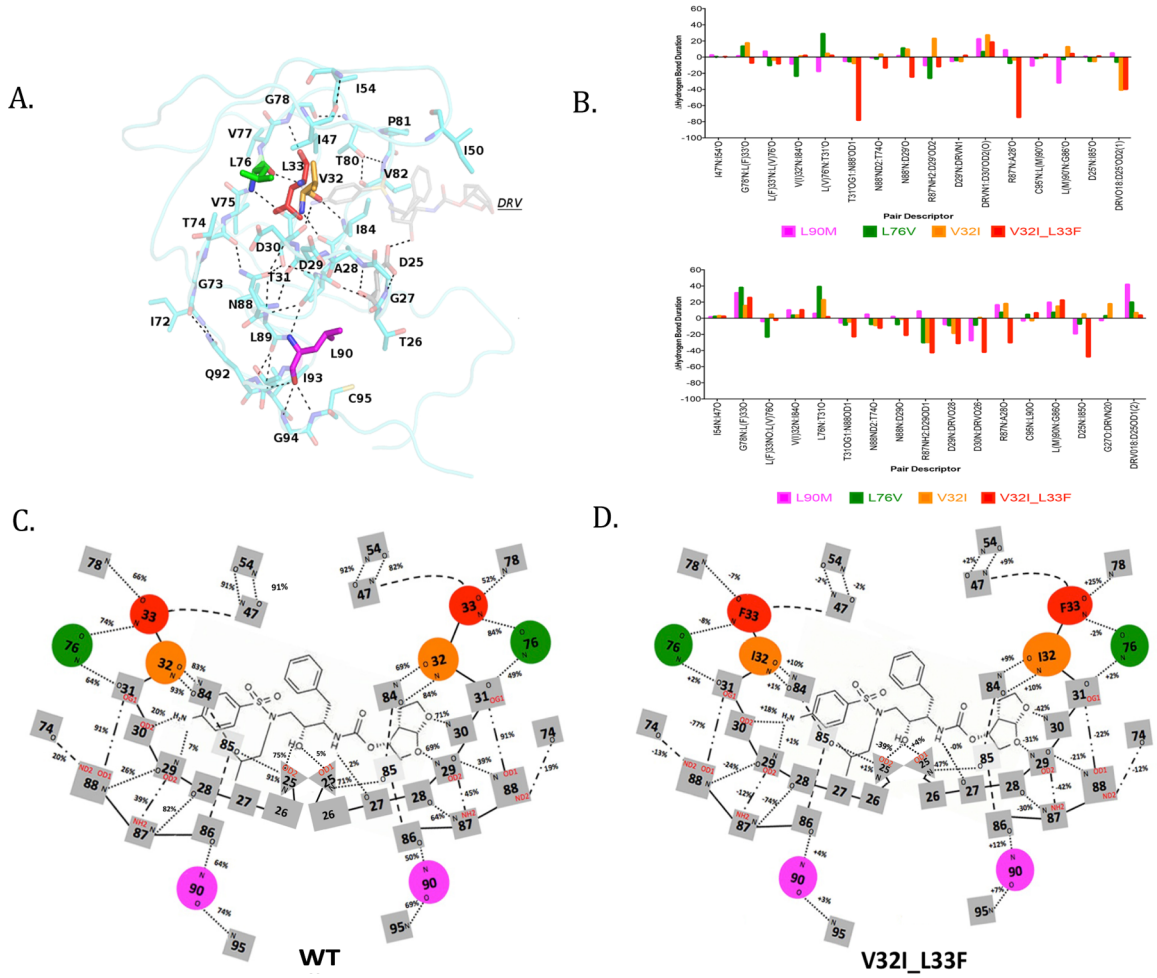

Figure 5. Network of hydrogen bonds within HIV-1 protease. (A) Crystal structure of DRV bound to the active site, and only one monomer of the protease is shown for clarity. The sites of mutation (L76, L90, V32, and L33) have colored side chains. (B) Histograms of the changes of the percentage time hydrogen bonds are formed relative to the WT simulation for each of the complexes. (C) Schematic hydrogen bond network of the HIV-1 protease dimer with the percentage time hydrogen bonds are formed during the WT simulation (Figure S4). (D) Schematic representation of the V32I_L33F complex simulation with the change in hydrogen bonding relative to the WT simulations. The remaining variants schematic are shown in Figure S5.

and thereby the contact of I47 with DRV. Taken together, one can decipher how contacts between protein and inhibitor are affected by these changes even for residues that are packed through vdW contacts or covalently linked along the backbone and are not directly involved in the hydrogen bonding network (Figure 5A and C).

DISCUSSION

HIV-1 protease evolves in complex combinations to evade inhibition, but still maintains biological function. The active site mutations have a relatively straightforward mechanism of disturbing the inhibition−function balance, which is effectively explained by the substrate envelope.[6] However, in highly resistant variants, active site mutations often coexist with mutations outside the active site. This is particularly necessary when resistance is achieved to the highly potent inhibitor DRV, which fits well within the substrate envelope. However, the role of these changes outside the active site has long been thought to be only in recovering viral fitness, or protease stability.

In the current study, we have primarily chosen enzyme variants that are associated with DRV resistance: L76V, V32I, and L33F.[21] Although L76V causes only a 1.5-fold decrease in DRV binding affinity (Table 1), this mutation is often observed in highly mutated DRV-resistant variants,[22,23] as well as variants with hyper-susceptibility to other PIs. L33F is a highly networked mutation co-occurring with many others in highly drug-resistant patient isolates, often together with V32I.[24] Therefore, comparison of V32I and the V32I/L33F double mutant permits the context-dependence of mutational effects in drug resistance. While not directly associated with DRV resistance, L90M is a canonical highly networked mutation that typically arises in multidrug resistant proteases. The large and rigid P1/P1′ moieties in NFV and SQV have been implicated in susceptibility to L90M, a feature lacking in DRV.[10] L90M has been found in more than half of patient isolates with at least one PI resistance substitution, and hence is often present in patients needing DRV-based salvage therapy.[24] Thus, elucidating the physical impact of these secondary mutations on DRV binding provides a detailed perspective on how the enzyme accommodates such frequently observed changes.

Specifically, we find that mutations outside the active site impact inhibitor binding thereby playing a direct role in conferring drug resistance. Compared to the WT complex, the

dx.doi.org/10.1021/ja504096m | J. Am. Chem. Soc. 2014, 136, 11956−11963

overall structure and backbone conformations are very similar in the cocrystal structures of the variant complexes. However, the mutations cause subtle but significant rearrangements in the structure to cause altered interactions with the bound inhibitor, as well as impacting the dynamic ensembles of these complexes. We had previously hypothesized[12] and tested[25] that alterations in the hydrophobic core of the enzyme could alter the conformational dynamic ensemble through changes in the hydrophobic sliding of internal residues potentially impacting drug resistance. This impact on dynamics is not localized to the points of mutation but would propagate throughout the enzyme. In the present study we hypothesize these mutations outside the active site share a common pathway of altering the overall enzyme dynamics and propagating their effects to the active site.

Although the resistance-associated mutations are located at a variety of positions in the protease and away from the active site, they all may utilize a common mechanism or pathway of altering the protease−inhibitor interactions. The mutations cause subtle changes through the repacking of the active site; in particular, these are observed in the crystal structures at residues 47, 50, and 84 in both monomers, and also observed in the MD analysis (Figure S6). Within the crystal structures of both the L76V and L90M complexes residue I47, which is located in the flap, loses contact with DRV. In contrast, in the V32I complex I47 contacts are retained, while this loss is restored when L33F occurs in V32I/L33F (these changes are also observed in subtle differences in the MD simulation Figure S6). Interestingly, V32I and I47V are the second most frequent pair of residues often found to coevolve, thus compensating for each other.[24] Mutations at I47, together with I54, which its backbone is hydrogen bonded with, is a major DRV resistance site. Among about 30 total active site residues that contact DRV, I47 is consistently the residue whose contacts are affected the most in L76V, L90M, and V32I/L33F variants (Figure S3). These results suggest that the interactions of residue 47 with inhibitors within the active site may represent a pivotal site in conferring drug resistance to PIs, and these interactions can be altered by changes propagated through the enzyme from remote sites.

In addition to repacking around the inhibitor in the crystal structures, the secondary mutations share a common pattern of altering the dynamic ensemble sampled by the protease, and the shape of the active site. Overall in the dynamic ensemble of the V32I and the V32I/L33F variants the active site is expanded, with the double mutant expanding the active site more, while L76V active site contracts and the L90M active site displays asymmetric changes. Hence, even though not located at the active site, mutations at all these remote sites affect the shape of the active site in the dynamic ensemble.

How are single mutations at a remote site able to alter interactions and dynamics of the active site with highly common molecular mechanisms? We propose a "network hypothesis" where the perturbation introduced by mutation of a distal residue is propagated to the active site through a network of interactions within the protease structure (Figure 5). The distal mutation sites we studied are all part of a hydrogen-bonded network connecting to the active site where the inhibitor binds. Our network hypothesis postulates that the mutations have similar effects and common mechanisms as they all cause a rearrangement of this same network. This hypothesis is supported by the alterations observed during the MD simulations in the stability of the hydrogen bonding networks (Figure 5), where changes propagate from residues 74−78 and 87−90, through 28−33, to 84−85 and 25. This altered interaction network includes repacking of the vdW contacts with residues 47 and 54, which are pivotal in linking the networked residues to the rearrangement of the flaps, residues 29 and 30 that directly hydrogen bond to DRV, and 82 and 84 that are key sites within the active site cavity. We hypothesize that all these are the active site residues where the impact of distal mutations is propagated as a common mechanism of resistance in all variants and their subtle rearrangements can cause inhibitor specific resistant changes.

These common mechanisms provide an explanation for why some mutations are redundant and thus are not observed together in patient sequences, while others are synergistic and occur together to confer higher levels of drug resistance as they impact one another at pivotal sites that confer resistance often through expanding the active site. This hypothesis does not exclude the possibility that some changes may still provide additional stability, increasing the combined fitness of the variants. Most significantly, our findings show that all of the mutations we have studied, although outside the active site, still directly alter the shape and flexibility of the active site, thus likely play a direct role in conferring resistance.

METHODS

Protease Gene Construction. Each of the four protease mutants was constructed using a standard site-directed mutagenesis protocol on a WT-HXB2 protease gene with a codon sequence optimized for *E. coli* expression. The WT PR gene contained the amino acid substitution Q7K to minimize the enzyme's autoproteolytic activity.

Protease Expression and Purification. Each PR mutant was expressed and purified as previously described.[26] Briefly, the mutant HIV-1 protease gene was cloned into the pXC-35 plasmid, which was then transformed into the TAP56 strain of *Escherichia coli*. Transformed cells were grown in 6 × 1 L cultures from which cell pellets were harvested 3 h after induction. The cell pellets were lysed and the protease was retrieved from inclusion bodies with 100% glacial acetic acid. The protease was separated from higher molecular weight proteins by size-exclusion chromatography on a Sephadex G-75 column. The purified protein was refolded by rapid dilution into a 10-fold volume of 0.05 M sodium acetate buffer at pH 5.5, containing 10% glycerol, 5% ethylene glycol, and 5 mM dithiothreitol (refolding buffer). The protease solution was concentrated, followed by dialysis to remove any remaining acetic acid. Protease used for crystallization was further purified with a Pharmacia Superdex 75 fast-performance liquid chromatography column equilibrated with refolding buffer.

Protease Crystallization. Crystals were set up with a 5-fold molar excess of inhibitor to protease, which ensures ubiquitous binding. The final protein concentration ranged from 0.8 to 1.6 mg/mL in refolding buffer. The hanging-drop method was used for crystallization as previously described.[26] For the L76V, L90M, and V32I mutants, the reservoir solution consisted of 126 mM phosphate buffer at pH 6.2, 63 mM sodium citrate, and ammonium sulfate at a range of 24−29%. For the V32I/L33F double mutant, the reservoir solution consisted of 0.1 M citrate-phosphate buffer, 7% DMSO, and 25−30% ammonium sulfate.

Enzyme Kinetics. Enzyme inhibition studies were carried out using a PerkinElmer Envision multilabel plate reader. A substrate peptide mimicking the MA-CA (p17-p24) cleavage site labeled with K-E(EDANS)-S-Q-N-Y-P-I-V-Q-K(DABCYL)-R (0.5 μM, final concentration) was added just prior to the reading to each well containing 50 nM of PR and varying concentrations of inhibitor. The FRET pair (EDANS, the donor and DABCYL, the quencher) was attached to the indicated amino acids of the peptide (Molecular Probes). Fluorescence intensity increase upon hydrolysis of the fluorogenic substrate was monitored at 490 nm (emission of EDANS) from the highest inhibitor concentration to the lowest, as well as the no inhibitor control well.

Each inhibitor titration included at least 12 inhibitor concentration points. Initial velocities were obtained from the progress curves and plotted against inhibitor concentration to get inhibition curves. Resulting curves were globally fitted to Morrison's equation to obtain the K_i value, as described previously.[27]

Evaluation of Hydrogen Bonding and van der Waals Interactions. The Maestro component of the Schröedinger software suite was used to analyze the hydrogen bonds between the inhibitor and the protease residues and neighboring waters after optimization of the complex structure. Briefly, a hydrogen bond was defined by a distance between donor and acceptor of <3.5 Å and a donor-hydrogen acceptor angle of >120°. The vdW contacts between the inhibitor and protease were calculated using a simplified Lennard−Jones potential, following previously published protocols.[28]

MD Simulations. The MD simulations were performed using the program Sander in the Amber 8 package, as previously described.[20] A set of three simulations was run for each of the four mutants and the WT-PR yielding a total of 15 trajectories for analysis. Each simulation was assigned initial velocities according to the Maxwellian distribution and random seeds were assigned with five different values for each PR. An in-house script was used to determine the intra and intermonomeric Cα distances between various residues using the trajectories. To calculate the hydrogen bond duration between various residues within the network from the simulations, the Visual Molecular Dynamics (VMD) version 1.9.1 was used.[29,30] VMD was used to write out the trajectory in a pdb format using the coordinates and trajectory files generated by PTraj from the AMBER simulation software. VMD was also used to generate the trajectory pdb files to determine the vdW contact energies over the simulations. The in-house vdW script was then modified to assess vdW contacts from the simulations. The script was run to determine vdW contacts for each of the trajectories. Once the robustness of the system was assessed, the three trajectories for each system were concatenated into one file containing 1500 frames and the total vdW contacts were analyzed.[31]

■ ASSOCIATED CONTENT

Supporting Information

Plots of vdW interaction energy of active site residues in crystal structures. Plots of distance distributions between residue pairs around the active site, histograms and schematics of hydrogen bonding networks and histograms of vdW from the five sets MD trajectories of DRV-bound HIV-1 protease complexes. This material is available free of charge via the Internet at http://pubs.acs.org.

■ AUTHOR INFORMATION

Corresponding Author

Celia.Schiffer@umassmed.edu

Notes

The authors declare no competing financial interest.

■ ACKNOWLEDGMENTS

We thank Shivender Shandilya and Aysegül Özen for technical assistance. This research was supported by National Institute of Health (NIH) Grants R01-GM65347, GM65347-12S1 supplement, and F31 GM111101 to D.A.R. This paper is dedicated to the late Bridgett Earlene Ragland.

■ REFERENCES

(1) Lefebvre, E.; Schiffer, C. A. *AIDS Rev.* **2008**, *10*, 131.
(2) Thompson, M. A.; Aberg, J. A.; Cahn, P.; Montaner, J. S.; Rizzardini, G.; Telenti, A.; Gatell, J. M.; Gunthard, H. F.; Hammer, S. M.; Hirsch, M. S.; Jacobsen, D. M.; Reiss, P.; Richman, D. D.; Volberding, P. A.; Yeni, P.; Schooley, R. T. *JAMA, J. Am. Med. Assoc.* **2010**, *304*, 321.
(3) Volberding, P. A.; Deeks, S. G. *Lancet* **2010**, *376*, 49.
(4) Rosenbloom, D. I.; Hill, A. L.; Rabi, S. A.; Siliciano, R. F.; Nowak, M. A. *Nat. Med.* **2012**, *18*, 1378.
(5) Wu, T. D.; Schiffer, C. A.; Gonzales, M. J.; Taylor, J.; Kantor, R.; Chou, S.; Israelski, D.; Zolopa, A. R.; Fessel, W. J.; Shafer, R. W. *J. Virol.* **2003**, *77*, 4863.
(6) King, N. M.; Prabu-Jeyabalan, M.; Nalivaika, E. A.; Schiffer, C. A. *Chem. Biol.* **2004**, *11*, 1333.
(7) Šašková, K. G.; Kožíšek, M.; Lepšík, M.; Brynda, J.; Rezácová, P.; Václavíková, .; Kagan, R. M.; Machala, L.; Konvalinka, J. *Protein Sci.* **2008**, *17*, 1555.
(8) Kovalevsky, A. Y.; Tie, Y. F.; Liu, F. L.; Boross, P. I.; Wang, Y. F.; Leshchenko, S.; Ghosh, A. K.; Harrison, R. W.; Weber, I. T. *J. Med. Chem.* **2006**, *49*, 1379.
(9) Louis, J. M.; Zhang, Y.; Sayer, J. M.; Wang, Y. F.; Harrison, R. W.; Weber, I. T. *Biochemistry* **2011**, *50*, 4786.
(10) Ode, H.; Neya, S.; Hata, M.; Sugiura, W.; Hoshino, T. *J. Am. Chem. Soc.* **2006**, *128*, 7887.
(11) Shen, C. H.; Wang, Y. F.; Kovalevsky, A. Y.; Harrison, R. W.; Weber, I. T. *FEBS J.* **2010**, *277*, 3699.
(12) Foulkes-Murzycki, J. E.; Scott, W. R.; Schiffer, C. A. *Structure* **2007**, *15*, 225.
(13) King, N. M.; Prabu-Jeyabalan, M.; Nalivaika, E. A.; Wigerinck, P.; de Bethune, M. P.; Schiffer, C. A. *J. Virol.* **2004**, *78*, 12012.
(14) Nalam, M. N.; Ali, A.; Altman, M. D.; Reddy, G. S.; Chellappan, S.; Kairys, V.; Ozen, A.; Cao, H.; Gilson, M. K.; Tidor, B.; Rana, T. M.; Schiffer, C. A. *J. Virol.* **2010**, *84*, 5368.
(15) Santos, J. R.; Molto, J.; Llibre, J. M.; Negredo, E.; Bravo, I.; Ornelas, A.; Clotet, B.; Paredes, R. *PLoS One* **2012**, *7*, e37442.
(16) Surleraux, D. L.; Tahri, A.; Verschueren, W. G.; Pille, G. M.; de Kock, H. A.; Jonckers, T. H.; Peeters, A.; De Meyer, S.; Azijn, H.; Pauwels, R.; de Bethune, M. P.; King, N. M.; Prabu-Jeyabalan, M.; Schiffer, C. A.; Wigerinck, P. B. *J. Med. Chem.* **2005**, *48*, 1813.
(17) Weber, I. T.; Agniswamy, J. *Viruses* **2009**, *1*, 1110.
(18) Cai, Y.; Myint, W.; Paulsen, J. L.; Schiffer, C. A.; Ishima, R.; Kurt Yilmaz, N. *J. Chem. Theory Comput.* **2014**, *10*, 3438.
(19) Cai, Y.; Schiffer, C. A. *J. Chem. Theory Comput.* **2010**, *6*, 1358.
(20) Cai, Y.; Yilmaz, N. K.; Myint, W.; Ishima, R.; Schiffer, C. A. *J. Chem. Theory Comput.* **2012**, *8*, 3452.
(21) de Meyer, S.; Vangeneugden, T.; van Baelen, B.; de Paepe, E.; van Marck, H.; Picchio, G.; Lefebvre, E.; de Bethune, M. P. *AIDS Res. Hum. Retroviruses* **2008**, *24*, 379.
(22) Wiesmann, F.; Vachta, J.; Ehret, R.; Walter, H.; Kaiser, R.; Sturmer, M.; Tappe, A.; Daumer, M.; Berg, T.; Naeth, G.; Braun, P.; Knechten, H. *AIDS Res. Ther.* **2011**, *8*, 7.
(23) Young, T. P.; Parkin, N. T.; Stawiski, E.; Pilot-Matias, T.; Trinh, R.; Kempf, D. J.; Norton, M. *Antimicrob. Agents Chemother.* **2010**, *54*, 4903.
(24) Varghese, V.; Mitsuya, Y.; Fessel, W. J.; Liu, T. F.; Melikian, G. L.; Katzenstein, D. A.; Schiffer, C. A.; Holmes, S. P.; Shafer, R. W. *Antimicrob. Agents Chemother.* **2013**, *57*, 4290.
(25) Mittal, S.; Cai, Y.; Nalam, M. N. L.; Bolon, D. N.; Schiffer, C. A. *J. Am. Chem. Soc.* **2012**, *134*, 4163.
(26) Prabu-Jeyabalan, M.; Nalivaika, E.; Schiffer, C. A. *J. Mol. Biol.* **2000**, *301*, 1207.
(27) Aydin, C.; Mukherjee, S.; Hanson, A. M.; Frick, D. N.; Schiffer, C. A. *Protein Sci.* **2013**, *22*, 1786.
(28) Ozen, A.; Haliloglu, T.; Schiffer, C. A. *J. Mol. Biol.* **2011**, *410*, 726.
(29) Hsin, J.; Arkhipov, A.; Yin, Y.; Stone, J. E.; Schulten, K. *Curr. Protoc. Bioinf.* **2008**, DOI: 10.1002/0471250953.bi0507s24.
(30) Humphrey, W.; Dalke, A.; Schulten, K. *J. Mol. Graphics* **1996**, *14*, 33.
(31) Amaro, R. E.; Swift, R. V.; Votapka, L.; Li, W. W.; Walker, R. C.; Bush, R. M. *Nat. Commun.* **2011**, *2*, 388.